

J. Y. Pastor

J. LLorca

J. Planas

M. Elices

Department of Materials Science,
Polytechnic University of Madrid,
28040-Madrid, Spain

Stable Crack Growth in Ceramics at Ambient and Elevated Temperatures

Quasi-static, stable crack propagation tests in ceramics are presented. The tests are performed using a recently developed technique in which the crack mouth opening displacement (CMOD) is continuously monitored during the test by means of a laser extensometer, and this signal is employed to control a servo-hydraulic testing machine. The advantages of such tests to characterize the fracture behavior of ceramics at high temperature are described, and the technique is used to study the fracture behavior of an yttria-partially stabilized zirconia ceramic at ambient and elevated temperatures.

Introduction

Monolithic ceramics have long been considered as ideal materials to apply fracture mechanics in its simplest form. It is often assumed that energy dissipation outside the crack tip region in ceramics is negligible, that the length of the fracture process zone around the crack tip is always small as compared with any characteristic dimension of the specimen, and that the crack propagated when the stress intensity factor at the tip reached a critical value, K_{Ic} . Under these circumstances, K_{Ic} is a *true* material property, independent of the specimen size, geometry, and loading conditions, which can be measured through a simple mechanical test on a precracked specimen from the peak load and the initial precrack length. However, a large number of experimental observations in recent years indicated that these hypotheses are not accurate for many monolithic ceramics and for most fiber-reinforced ceramic composites, the differences increasing with the toughness of the material. In ceramics toughened by crack wake interactions, the fracture process zone can reach several millimeters in length, being comparable to the specimen unbroken ligament and to the initial crack length, and the peak load might not be attained until substantial subcritical crack growth has taken place. The material growth resistance is no longer constant, and it increases with crack length (R-curve) until a steady-state value is reached if the specimen is large enough (Bazant and Kazemi, 1990; LLorca and Elices, 1992). Moreover, the apparent fracture toughness of the material (obtained from the peak load and the initial precrack length) becomes dependent on the specimen size and geometry and cannot be considered a material property. Similar R-curve effects appear in transforming ceramics, where the crack growth resistance increases with the applied stress intensity factor as the crack grows and more material in front of the crack tip undergoes the tetragonal

to monoclinic symmetry transformation (Evans and Cannon, 1986). In addition, nonlinear deformations may occur in the bulk material at high temperatures, and the energy spent to propagate the crack has to be separated from that dissipated in the bulk to obtain an accurate estimation of the influence of temperature on the crack growth resistance.

The search for better parameters to characterize the fracture behavior of ceramics and the underlying mechanisms have been linked to the development of quasi-static, stable crack propagation tests, where the complete load-displacement curve is obtained. For instance, when the only mechanism of energy dissipation is friction in the crack wake, the material fracture energy can be obtained as the energy employed to break the specimen per unit crack area, and this magnitude is a *true* material property in the sense that it does not depend on extrinsic factors such as specimen size or geometry (Elices and Planas, 1989). Moreover, stable fracture tests provide the possibility of computing the complete R-curves. Stable crack propagation tests in ceramics are difficult to carry out because the high stiffness of these materials, which is higher than that of the testing machine, and usually leads to the catastrophic propagation of the crack beyond the peak load under crosshead displacement control. This paper presents the results of stable crack propagation tests in ceramics at both room and high temperatures. The tests are obtained using a recently developed method based on measuring the crack mouth opening displacement (CMOD) through a laser extensometer, and using this signal to drive a servo-hydraulic testing machine in real time during the test. Since the CMOD increases monotonically with crack length, this system enables stable crack growth tests to be carried out in any typical geometry used in fracture testing, and it is especially suitable for high temperatures. The specific features of this method are compared with other high temperature fracture testing methods, and the technique is employed to study the fracture behavior of a $ZrO_2/3.0$ percent mol. Y_2O_3 (Y-PSZ) ceramic in the temperature range 25 to 600°C.

Contributed by the Materials Division and presented at the Symposium on Micromechanics of Ceramics and Ceramic Composites, Winter Annual Meeting, Anaheim, CA, November 8-13, 1992, of THE AMERICAN SOCIETY OF MECHANICAL ENGINEERS. Manuscript received by the Materials Division May 10, 1992; revised manuscript received December 9, 1992. Associate Technical Editor: S. Suresh.

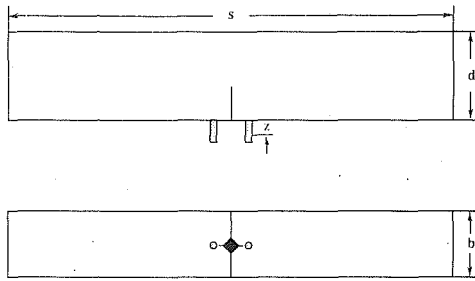


Fig. 1 Specimen notation

Material and Experimental Techniques

A commercially available yttria-partially stabilized zirconia (3.0 mol. percent Y-PSZ) supplied by Ceraten, S. A. (Madrid, Spain) was used in this investigation. The powders were cold isostatically pressed into rectangular plates ($100 \times 50 \times 10 \text{ mm}^3$) at 170 MPa, and then sintered at 1500°C for 2 hours. The sintered material contained monoclinic and tetragonal phases with volume fractions of 26 and 74 percent, respectively. Grain size distribution was determined by scanning electron microscopy of polished surfaces, which were thermally etched at 1350°C for 30 minutes. The average grain size is $0.34 \mu\text{m}$, and sixty percent of the grains are below $1 \mu\text{m}$. Only ten percent of the grains are larger than $6 \mu\text{m}$.

The plates were machined into rectangular bars, dimensions $50 \times 10 \times 5 \text{ mm}^3$, which were precracked to obtain single edge precracked beam specimens using the bridge indentation or compression method (Warren and Johannesson, 1984; Nose and Fujii, 1988). In this method, a Vickers indentation was placed as a crack starter at the center of the bottom surface of the beam. The beam was then sandwiched by a flat pusher and a very rigid and hard metallic anvil with a central groove. The indentation was aligned with the center of the groove, and the specimen was loaded in compression in a hydraulic machine until a pop-in sound was detected, indicating that a through-thickness crack was propagated from the crack starter. Straight through-thickness cracks with a length between 3.5 to 6.5 mm were obtained with this method.

The measurement of the CMOD during the test was performed by a scanner laser beam. To this end, two small alumina pins were glued with a refractory cement to the bottom of the specimen at both sides of the crack mouth (Fig. 1). The separation between the pins was 1.5 mm. Afterwards, the cement was cured for 1 hour at 300°C , and the specimen was placed on a SiC three-point bend testing fixture, with a loading span of 40 mm. The specimen and the fixture were placed in the high temperature furnace and were loaded through two alumina rods connected to the actuators and to the load cell of a servo-hydraulic testing machine. The external ends of the rods were water-cooled to avoid overheating of the piston and the load cell.

The laser extensometer is essentially the same as the one reported by Carroll et al. (1989); it consists of a detector and He-Ne laser that scanned in a horizontal line over 150 times per second. The laser was directed through a silica glass window in the furnace towards the two pins glued to the specimen. The ceramic cement employed is able to provide a good adhesion up to 1600°C . The detector was located in front of the laser, and received the laser beam through another silica glass window after passing between the pins. The two ceramic pins were chosen of cylindrical shape to avoid errors in the measurement due to misalignments among the pins, the specimen, and the laser beam, as could happen with square pins. A multidimensional measurement processor reads the signal in the detector and calculates the separation between the pins. The accuracy of the extensometer depends on the noise produced by density fluctuations in the laser path. At high tem-

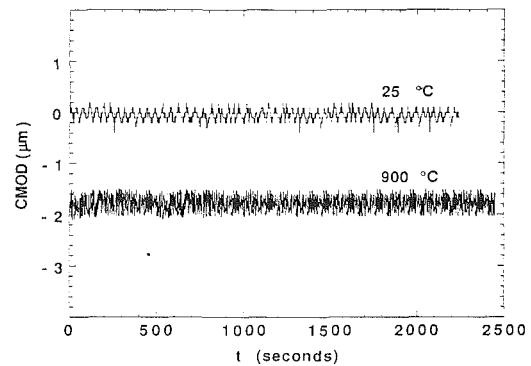


Fig. 2 Fluctuations of CMOD measurements at 25 and 900°C . The stepped appearance of the trace for 25°C is due to setting the digital-to-analog converter to a $0.1 \mu\text{m}$ resolution, while the resolution at 900°C was set to $0.01 \mu\text{m}$. The output resolution is user-set, and does not affect the internal digital resolution.

peratures, Carroll et al. (1989) identified two main sources of noise, produced by the air seepage around the loading rods and by thermal gradients along the optical path. Preliminary calibrations of the extensometer indicated that air seepage was dominant as compared with the thermal gradients in our system, perhaps because the large size of the furnace led to smaller temperature gradients along the laser path. Thus special care was taken to reduce the chimney effect as much as possible by closing the gaps between the loading rods and the furnace, and the specimen remained at the test temperature for one hour before testing to achieve a stationary distribution of temperatures within the furnace. Moreover, the good thermal insulation of the furnace allowed the laser source and detector to be located very close to the silica glass without danger of their overheating, reducing the fluctuations produced outside the furnace. In addition to all these precautions, the measurements were averaged over 150 scans for each displacement to minimize the noise. This averaging procedure was also recommended by Carroll et al. (1989) who found that the accuracy of the system improved with the number of scans used to obtain one single measurement. However, as the CMOD measurements are employed to control the testing machine, the maximum number of scans used to produce one CMOD value should be reduced to a minimum. Otherwise the testing machine is not able to respond quickly enough to the changes in specimen compliance when the crack starts to propagate around the peak load, and catastrophic failure takes place. By reducing the noise sources as mentioned above, it was possible to reduce the fluctuations in the measurements to the levels shown in Fig. 2, and also to obtain stable fracture tests. According to these results, the standard deviation of the measurements over a period of forty minutes is about $\pm 0.2 \mu\text{m}$ both at ambient temperature and at 900°C . A typical fracture test took about 35 minutes.

Samples were tested at 25, 300 and 600°C . In the high temperature tests, the specimens were placed in the bending fixture, slightly preloaded, and heated at a rate of 8°C per minute under constant load. After stabilizing the temperature for one hour, the machine control was transferred to CMOD, as supplied by the analog output of the laser extensometer. The details of the feed-back set up and the analysis of the performance of the control will be given elsewhere. During the test an automatic data acquisition system read load, CMOD and deflection at one second intervals. The CMOD rate was $1 \mu\text{m}$ per minute. This low loading rate was selected in order to assure the stability of the test. The deflection of the loading system was measured by a LVDT transducer outside the furnace.

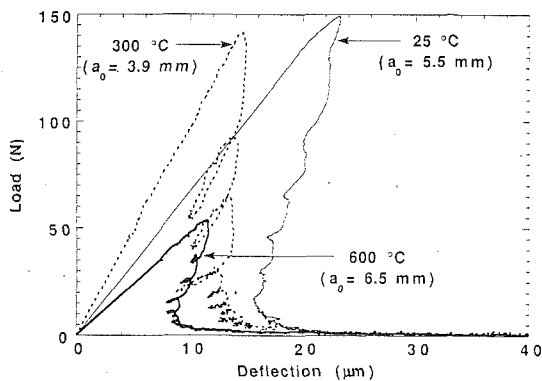


Fig. 3 Load-deflection curves at 25, 300, 600°C. The initial crack length, a_0 , in each test is also shown between parentheses.

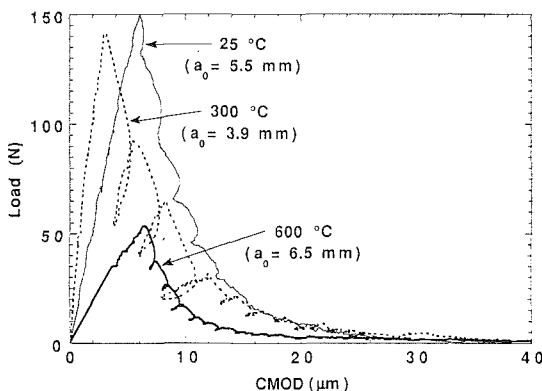


Fig. 4 Load-CMOD curves at 25, 300, 600°C. The initial crack length, a_0 , in each test is also shown between parentheses.

Results and Discussion

Typical load-deflection and load-CMOD curves obtained from the CMOD-controlled tests are shown respectively in Figs. 3 and 4 for tests carried out at 25, 300, and 600°C. The load-deflection curves present a snap-back behavior beyond the peak load at all temperatures, and they would be unstable if the tests were performed under cross-head displacement control. Actually, all the tests carried out under this latter type of control failed catastrophically beyond the peak load. This problem is associated with the high stiffness of ceramics, which is usually higher than that of the testing rig. The difficulties of obtaining stable tests in ceramic materials have led to the characterization of their fracture behavior through the apparent fracture toughness, which can be measured in unstable tests. This magnitude, however, may be dependent on specimen geometry and size, the differences increasing with the material toughness, and it is not suitable for characterizing the behavior of the new families of tough ceramics currently under development (Heuer, 1987). Several experimental techniques have been proposed recently to improve the stability of fracture tests on ceramics. The first group of techniques is based on increasing the stiffness of the testing system by using ceramic loading devices (Wieninger et al., 1986), and reducing the stiffness of the specimen with deep precracks. Another method uses Chevron-notched bend bars, which display considerable subcritical crack growth prior to reaching the peak load, as the crack area increases linearly with crack length (Ghosh et al., 1989; 1991). Finally, Maniette et al. (1991) used a C-clamp on a compact tension specimen. The stiffness of the clamp is connected in parallel with the specimen and this improves the stability of the fracture test.

At high temperatures, however, the measurement of defor-

Table 1 Experimentally measured G_F , K_{∞} , and K_{IQ} as a function of the temperature in Y-PSZ

Temperature (°C)	G_F (J/m ²)	K_{∞} (MPa m ^{1/2})	K_{IQ} (MPa m ^{1/2})
25	53.6	3.7	3.6
300	35.4	2.7	2.4
600	21.2	2.1	2.1

mation is another difficult task. It should be noted that in order to obtain the R-curve it is not enough to get stable fracture tests, but it is also necessary to monitor continuously either the crack length or another parameter which is related to it. The CMOD, which is very sensitive to the changes in crack length, is often used to this end in fracture experiments, and the relationship between both magnitudes is available in the handbooks for the majority of specimens used in fracture testing. The use of laser-based extensometers has become very popular in recent years to monitor displacements in ceramics at high temperature, where a high resolution is required and the extensometer cannot be in contact with the specimen (Jenkins et al., 1987; Carroll et al., 1989; Geiger, 1990; Baxter, 1991).

The experimental technique presented in this paper presents the advantage that the laser extensometer allows the CMOD measurement, and this output is employed simultaneously to control the testing machine, leading to stable crack propagation tests in which all relevant fracture parameters can be obtained. Although this method can be used at ambient and elevated temperatures, its primary field of application is found in the latter, where laser extensometers exhibit very important advantages (Geiger, 1990; Baxter, 1991).

From the load-deflection curves in Fig. 3, the fracture energy, G_F , can be calculated by dividing the energy spent to break the specimen by the crack surface increment during the test. The results are given in Table 1 for the three different temperatures tested. From these values, the fracture toughness for an infinite size specimen, K_{∞} , is readily obtained as

$$K_{\infty} = \sqrt{G_F E} \quad (1)$$

where the Young's modulus, E , is determined in each specimen from the initial slope of the P-CMOD curve and the initial precrack length measured on the crack surface once the specimen is broken. Mathematically,

$$E = \frac{P}{\text{CMOD}} \frac{6sa_0^*}{bd^{*2}} V_1 \left[\frac{a_0^*}{d^*} \right] \quad (2)$$

where s is the span of the three-point bend fixture, b the specimen thickness, and V_1 is a nondimensional function found in the literature for this geometry (Tada et al., 1985). The magnitudes a_0^* and d^* stand for the corrected values of the initial crack length and beam depth respectively. This correction is needed because the laser measurement of the CMOD is not done exactly at the crack mouth, but at a distance z below it (Fig. 1). A simple way of taking this fact into account is using $a_0^* = a_0 + z$ and $d^* = d + z$ in Eq. (2) instead of a and d .

The apparent fracture toughness, K_{IQ} , obtained from the peak load and the initial crack length, is shown in Table 1 as well. They exhibit good agreement with K_{∞} values, indicating that for this material and temperature range $K_{IC} \approx K_{IQ} \approx K_{\infty}$ is a valid parameter to characterize the fracture behavior. Scanning electron microscopy of the fracture surfaces revealed that crack propagation was mainly transgranular and that the porosity of the material was significant (Fig. 5).

The crack growth resistance, K_R , can also be obtained from the P-CMOD curves by assuming that the bulk material behaves as a linear elastic solid during deformation, and defining an equivalent elastic crack length. If the fracture process zone is small, the P-CMOD curve upon unloading goes through the

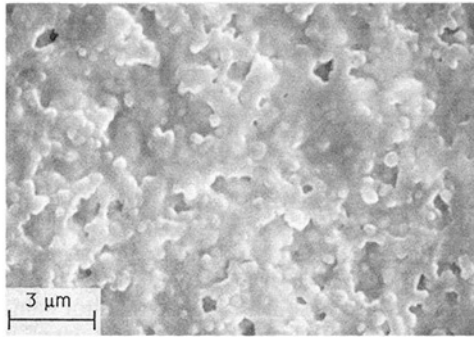


Fig. 5 Aspect of the fracture surface in Y-PSZ, showing transgranular fracture and porosity

origin of coordinates, and the equivalent elastic crack length can be calculated from Eq. (2). K_R is then obtained from the load P and the equivalent crack length through standard expressions available in the handbooks. For the materials and temperatures tested, this approach seems to be accurate because the P-CMOD curves were almost linear up to the peak load, and controlled unloadings carried out during the tests were directed towards the origin (Fig. 4).

The K_R versus a curves are plotted in Fig. 6 for the three temperatures. Crack propagation was detected only beyond a certain value of the applied stress intensity factor due to the precracking method, which involves the stable growth of the crack from the Vickers indentation. Under these circumstances, the material transformed around the crack tip during indentation increases the initial crack growth resistance of the material, and crack propagation is not started until a minimum value of the applied stress intensity factor is reached. The R-curves at 25 and 600°C are almost flat, although the crack growth resistance tends to decrease slightly with crack length,¹ whereas the R-curve at 300°C exhibits a slight positive slope. The K_∞ values at each temperature are also plotted in Fig. 6 as horizontal lines. K_∞ can be interpreted as the crack growth resistance of a propagating steady-state crack within an infinite size specimen. The good agreement between the R-curve and K_∞ indicates that the crack propagates in a steady-state condition through the three-point bend beam. Marshall et al. (1983) pointed out that the steady-state crack growth regime is attained in transforming ceramics when the crack propagates a distance of over five times h , h being the length of the zone at the crack tip in which the tetragonal to monoclinic transformation occurs. An estimation of h is given by McMeeking and Evans (1982) according to

$$h = \left[\frac{\Delta K}{A V_f E \epsilon^T} \right]^2 \quad (3)$$

where $A = 0.22/(1 - \nu)$ for a purely dilatational supercritical transformation driven by the hydrostatic stresses, V_f is the volume fraction of transformed tetragonal phase, ϵ^T stands for the unconstrained dilatational strain, and ΔK represents the increase in toughness due to the transformation. It was shown that h decreases as the critical hydrostatic stress for transformation increases (Evans and Cannon, 1986), and thus the transformed zone will be maximum at room temperature because the transformation stress grows with the temperature. By choosing the appropriate values for each one of these mag-

¹Stump and Budiansky (1989) studied theoretically the R-curve behavior of transformation-toughened ceramics undergoing a uniform dilatational phase transformation. In their study, a semi-infinite crack was propagated at a constant stress intensity factor at the crack tip, and the evolution of the transformed zone around the advancing crack tip was taken into account. It was found that maximum toughening was obtained for finite amounts of crack advance, and the theoretical R-curves exhibited a shape similar to those in Fig. 6.

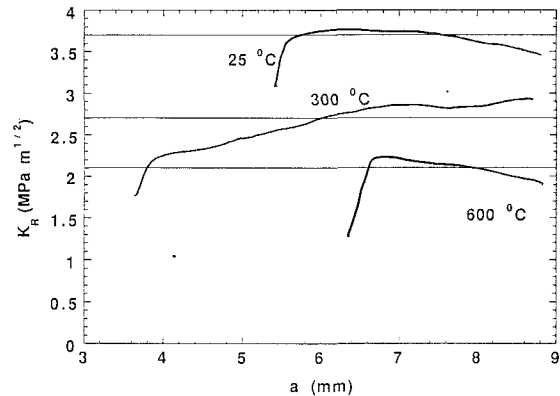


Fig. 6 R-curves obtained from the stable crack propagation tests in Y-PSZ at different temperatures. The horizontal lines stand for the fracture toughness obtained from the fracture energy measurements at each temperature.

nitudes ($V_f = 0.74$, $E = 200$ GPa, $\nu = 0.3$, $\epsilon^T = 0.04$) (Swain, 1985), and assuming that phase transformation is the main mechanism of toughening (thus, $\Delta K \approx K_\infty$), an upper boundary of $4 \mu\text{m}$ for h at 25°C can be obtained. As the temperature increases, the critical stress for transformation rises, the size of the transformed zone around the crack tip diminishes. Thus, the steady-state situation is reached very early during crack propagation, and most crack growth takes place under constant crack growth resistance conditions. Moreover, h is negligible as compared to the specimen characteristic dimensions even for very long cracks ($a/d \approx 0.9$), and size and geometry effects are not expected to be significant.

It is worth noting that the R-curve and K_∞ were obtained separately, the former from the P-CMOD curve and the latter from the area under the load-deflection curve. When linear elastic fracture mechanics applies, and the size of the fracture process zone is small, both approaches lead to equivalent results, and the R-curve is flat, with a constant value given by K_∞ or K_{IC} . However, this is not true in ceramics when the length of the process zone, where energy dissipation takes place, is not negligible. Examples of this behavior are found in very high-toughness transformation toughening ceramics (Inghels et al., 1990), and in coarse grain size monolithic ceramics, where grain bridging and grain interlocking lead to process zones of several millimeters in length (Wieninger et al., 1986; LLorca and Steinbrech, 1991). Under these circumstances, stable crack propagation tests are needed to fully characterize the fracture behavior.

Conclusions

1. A laser extensometer may be used advantageously to perform stable crack propagation tests in ceramics at ambient and elevated temperatures.
2. Stable fracture tests supply much more information than classical up-to-peak tests. In particular, the fracture energy and the R-curve may be determined in addition to the apparent fracture toughness.
3. The results for Y-PSZ ceramic in the range of temperatures from 25 to 600°C show that the R-curves are essentially flat, and that the apparent fracture toughness is close to the fracture toughness derived from the fracture energy measurement.
4. The above results indicate that small scale yielding conditions are met for this material and for the specimen size used, and a classical LEFM criterion may be used for crack propagation. However, stable fracture tests could be used to characterize materials with a strongly non-linear fracture response, due either to bulk non-linear behavior or to crack bridging stresses.

Acknowledgments

This research was supported by the Interdepartmental Commission for Science and Technology (CICYT) of Spain under grant number MAT90-1153-E.

References

- Baxter, D. F., 1991, "Tensile Testing at Extreme Temperatures," *Advanced Mat. & Process.*, pp. 22-30.
- Bazant, Z. P., and Kazemi, K. T., 1990, "Size Effect in Fracture of Ceramics and its Use to Determine Fracture Energy and Effective Process Zone Length," *J. Am. Ceram. Soc.*, Vol. 73, pp. 1841-1856.
- Stump, D. M., and Budiansky, B., 1989, "Crack-Growth Resistance in Transformation-Toughened Ceramics," *Int. J. Solids Structures*, Vol. 25, pp. 635-646.
- Carroll, D. F., Wiederhorn, S. M., and Roberts, D. E., 1989, "Technique for Tensile Creep Testing of Ceramics," *J. Am. Ceram. Soc.*, Vol. 72, pp. 1610-1614.
- Elices, M., and Planas, J., 1989, "Material Models," Chapter 3, *Fracture Mechanics of Concrete Structures*, Elfgren, L., ed., Chapman & Hall, London, pp. 16-66.
- Evans, A. G., and Cannon, R. M., 1986, "Toughening of Brittle Solids by Martensitic Transformations," *Acta Metall.*, Vol. 34, pp. 761-800.
- Geiger, G., 1990, "Advancements in Mechanical Testing of Advanced Ceramics," *Ceram. Bull.*, Vol. 69, pp. 1793-1800.
- Ghosh, A., Jenkins, M. G., White, K. W., Kobayashi, A. S., and Bradt, R. C., 1989, "Elevated Temperature Fracture Resistance of a Sintered α -Silicon Carbide," *J. Am. Ceram. Soc.*, Vol. 72, pp. 242-247.
- Ghosh, A., White, K. W., Jenkins, M. G., Kobayashi, A. S., and Bradt, R. C., 1991, "Fracture Resistance of a Transparent Magnesium Aluminate Spinel," *J. Am. Ceram. Soc.*, Vol. 74, pp. 1624-1630.
- Heuer, A. H., 1987, "Transformation Toughening in ZrO₂-Containing Ceramics," *J. Am. Ceram. Soc.*, Vol. 70, pp. 689-698.
- Inghels, E., Heuer, A. H., and Steinbrech, R. W., 1990, "Fracture Mechanics of High-Toughness Magnesia-Partially Stabilized Zirconia," *J. Am. Ceram. Soc.*, Vol. 73, pp. 2023-2031.
- Jenkins, M. G., and Kobayashi, A. S., Sakai, M., White, K. W., and Bradt, R. C., 1987, "Fracture Toughness Testing of Ceramics Using Laser Interferometric Strain Gage," *Am. Ceram. Soc. Bull.*, Vol. 66, pp. 1734-1738.
- LLorca, J., and Elices, M., 1992, "On the Size Effect in Fracture of Ceramic-Ceramic Composite Materials," *Fracture Mechanics of Ceramics*, Vol. 9, Bradt, R. C. et al., ed., Plenum Press, pp. 53-68.
- LLorca, J., and Steinbrech, R. W., 1991, "Fracture of Alumina: An Experimental and Numerical Study," *J. Mater. Sci.*, Vol. 26, pp. 6383-6390.
- Maniette, Y., Inagaki, M., and Sakai, M., 1991, "Fracture Toughness and Crack Bridging of a Silicon Nitride Ceramic," *J. Europ. Ceram. Soc.*, Vol. 7, pp. 255-263.
- Marshall, D. B., Drory, M. D., and Evans, A. G., 1983, "Transformation Toughening in Ceramics," *Fracture Mechanics of Ceramics*, Vol. 6, Bradt, R. C. et al., ed., pp. 289-307, Plenum Press.
- McMeeking, R. M., and Evans, A. G., 1983, "Mechanics of Transformation-Toughening in Brittle Materials," *J. Am. Ceram. Soc.*, Vol. 65, pp. 242-246.
- Swain, M., 1985, "Inelastic Deformation of Mg-PSZ and Its Significance for Strength-Toughness Relationship of Zirconia Toughened Ceramics," *Acta Metall.*, Vol. 33, pp. 2083-2091.
- Nose, T., and Fujii, T., 1988, "Evaluation of Fracture Toughness for Ceramic Materials by a Single-Edge-Pre-cracked-Beam Method," *J. Am. Ceram. Soc.*, Vol. 71, pp. 328-333.
- Tada, H., Paris, P., and Irwin, G., 1985, "The Stress Analysis of Cracks Handbook," Del Research Corporation.
- Warren, R., and Johannesson, B., 1984, "Creation of Stable Cracks in Hardmetals Using Bridge Indentation," *Powder Metall.*, Vol. 27, pp. 25-29.
- Wieninger, H., Kromp, K., and Pabst, R. F., 1986, "Crack Resistance Curves of Alumina and Zirconia at Room Temperatures," *J. Mater. Sci.*, Vol. 21, pp. 411-418.